Fibers and Polymers 2004, Vol.5, No.4, 259-263

Acoustic Emission on Failure Analysis of Rubber-Modified Epoxy Resin

Deok-Bo Lee*

Reliability Analysis Research Center, Hanyang University, Seoul 133-791, Korea
(Received November 24, 2002; Revised July 30, 2004; Accepted September 10, 2004)

Abstract: Rubber-modified epoxy resins have been employed as adhesive and matrix materials for glass and corbon-fiber composites. The behavior of fracture around a crack tip for rubber-modified epoxy resin is investigated through the acoustic emission (AE) analysis of compact tension specimens. Damage zone and rubber particles distributed around a crack tip were observed by a polarized optical microscope and an atomic force microscope (AFM). The damage zone in front of pre-crack tip in rubber-modified specimen (15 wt% rubber) began to form at about 13 % level of the fracture load and grew in size until 57 % load level. After that, the crack propagated in a stick-slip manner. Based on time-frequency analysis of AE signals and microscopic observation of damage zone, it was thought that AE signals with frequency bands of 0.15-0.20 MHz and 0.20-0.30 MHz were generated from cavitation in the damage zone and crack propagation, respectively.

Keywords: Acoustic emission, Time-frequecy analysis, Fracture energy, Damage zone, Rubber-Modified Epoxy Resin, Fracture Toughness, Toughening mechanism, Rubber Particle

Introduction

Epoxy resin has superior mechanical properties and is widely used in engineering components as adhesive, matrix material of fiber reinforced composites and electronic package materials. However, the neat epoxy resin has poor resistance against the brittle fracture. Many researchers have improved the tough mechanism of epoxy by blending with particles, fibers and rubber etc. [1-7]. Rubber-modified epoxy resins with rubber contents of 10-20 wt% [1-5, 8-14] have been applied to many structural components for high fracture toughness. For the damage zone being formed around pre-crack tip in rubber-modified epoxy resin, Lee *et al.* [8-14] studied on the relationship between a damage zone around a crack tip and the fracture toughness of a rubber-modified epoxy resin under mode I and mixed-mode conditions. They showed that the fracture toughness, *Gc* of the modified epoxy resin was closely related to the area of damage zone. Pearson and Yee [15] and Bagheri and Pearson [16] discussed effects of both the size and the distribution of rubber particles inside the damage zone in the vicinity of pre-crack tip. Yee *et al.* [17] also investigated the growth of a damage zone around a notch tip of a toughened epoxy resin using the four-point bending tests of symmetrical double-edge double-notched (SDEDN) specimens. They showed that cavitation inside the damage zone caused local constraint relief in the resin, which delayed the initiation of crack in the matrix and allowed more plastic deformation. These studies of damage zones around crack tips were performed mostly to identify a toughening mechanism or elucidate the role of cavitation for rubber-modified epoxy resins under mode I and mixed-mode loading.

In this study, the growth process of damage zone in front of pre-crack tip in rubber-modified epoxy resin is analyzed by using the acoustic emission (AE) measurement. The damage zone and the rubber particles distributed around the crack tip are also observed by a polarized optical microscope and an atomic force microscope (AFM) for identification of AE source mechanisms of fracture.

*Corresponding author: leetokbo@hanyang.ac.kr

Experimental Procedure

Preparation of Materials and Specimens

The neat epoxy resin prepared for this study was diglycidyl ether of bisphenol A (AER250, Japan Nagase-Ciba Co.). An anaromatic amine (HY956, Japan Nagase-Ciba Co) was used as a curing agent. Liquid copolymer (CTBN 1300 x 8, UBE industries) of butadiene and acrylonitrile with a carboxyl end group was used as rubber. To make a rubber-modified epoxy resin, the CTBN was first added to the epoxy resin and mixed at 200-300 rpm for 10 min in a vacuum container. After that, the curing agent was mixed to the compound by hand for 10 min in the vacuum container. The rubber-epoxy mixture was finally poured into a pre-heated mold. This mold was kept to 120 °C for 16 hours to cure the rubber-modified epoxy. The unmodified epoxy resin was also made according to the same curing condition as above. The geometry of pure epoxy and the modified epoxy resin was of plate 5 mm in thickness. The rubber-modified epoxy resins consisted of 100 parts by weight of resin (wt%), 5 wt% piperidine and 5 and 15 wt% CTBN. Table 1 shows the composition and designation of various epoxy resins. The material properties

Table 1. Composition of various epoxy resins

Resin system	Designation	Composition (wt%)		
		Epoxy	CTBN	Piperidine
AER250	AER250	100	0	5
	AER250-5	100	5	5
	AER250-15	100	15	5

Table 2. Material properties of neat and rubber-modified epoxy resins

Resin system	Young's modulus E (GPa)	Poisson's ratio
AER250	3.84	0.31
AER250-5	3.60	0.33
AER250-15	2.58	0.37

of the neat and the rubber-modified epoxy resins are shown in Table 2.

Fracture Test and Acoustic Emission Measurement

The tensile test was performed at room temperature. The cross-head speed was kept constant at 1 mm/min. The geometry of the compact tension (CT) specimen for this study is shown in Figure 1. A pre-notch was machined at the edge of the specimen using a circular saw for V-notching and an initial crack was introduced to sharpen the notch tip by pushing a razor blade through the notch bottom [11].

Figure 2 shows schematic diagram for AE measurement during the bending test. AE signals were measured using the Mistras 2001 system (Physical Acoustic Corp.). AE sensor (FM-1, Englewood, Co.: detectable frequency range 100 kHz-1 MHz) was mounted on the surface near to the notch. The signals were amplified by an amount 40 dB using pre-amplifier and converted to digital signals through A/D converter in Mistras 2001 board. The threshold voltage in this study was 28 dB.

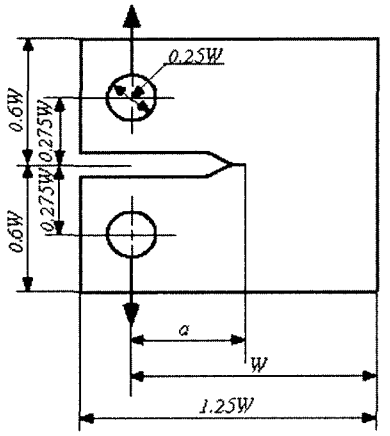

Figure 1. Compact tension specimen (w = 24 mm, a/w ≒ 0.5).

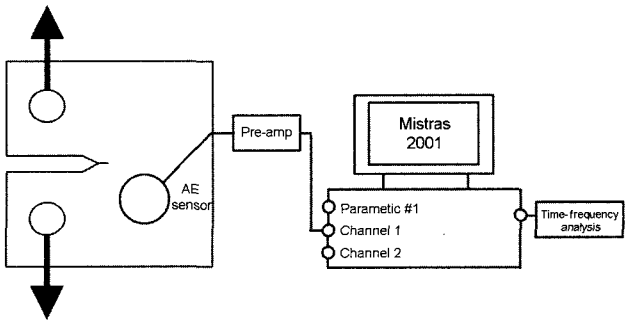

Figure 2. Schematic diagram of acoustic emission (AE) measurement.

Microscopic Fractography

A petrographic polishing technique was employed to investigate the damage zone around the pre-crack tip and the deformation of rubber particles in the damage zone. The details of this technique have been published by Holik *et al.* [18]. The technique is briefly explained as follows.

The specimens were loaded to 95 % of the maximum load. A section in the vicinity of damaged specimen is cut out using a low-speed diamond saw (ISO 9001 Resistered Co.). The section taken from the damaged specimen is potted in a clear epoxy resin which cures at room temperature. The surface of this sample is ground and finely polished using alumina powder. Then, the surface of the polished sample is mounted onto a clean slide glass using clear epoxy resin adhesive. This sample is allowed to cure overnight at room temperature. Excess resin is removed using the diamond saw, and the sample is again ground and polished until the plane of interest is finally reached. To best observe dispersed particles in the matrix resin, the thin section should be 20-200 μm thick. In this study, we polished the samples down to about 100 μm to measure the damage zone. A thinner sample is needed to observe the shapes of individual rubber particles, so the sample was polished again, this time as thin as possible (about 20 μm). All samples in this study were observed using a polarizing transmission optical microscopy and an atomic force microscopy (AFM).

Results and Discussion

Fracture Toughness

Fracture toughness (K_{IC}) was calculated in accordance with the ASTM specification (E399).

The stress intensity factors were given by

$$K_{IC} = X \cdot Y \cdot a^{1/2} \ [\mathrm{MPa \cdot m^{1/2}}]$$

$$X = \frac{P_c}{BW}$$

$$Y = \left(\frac{W}{a}\right)^{1/2} \times \frac{\left(2+\frac{a}{W}\right)}{\left(1-\frac{a}{W}\right)^{3/2}} \times \left\{0.886 + 4.64\left(\frac{a}{W}\right) - 13.32\left(\frac{a}{W}\right)^2 + 14.72\left(\frac{a}{W}\right)^3 - 5.6\left(\frac{a}{W}\right)^4\right\} \quad (1)$$

where B, W, a, and P_C are the thickness, the width, the length of notch and the critical load, respectively.

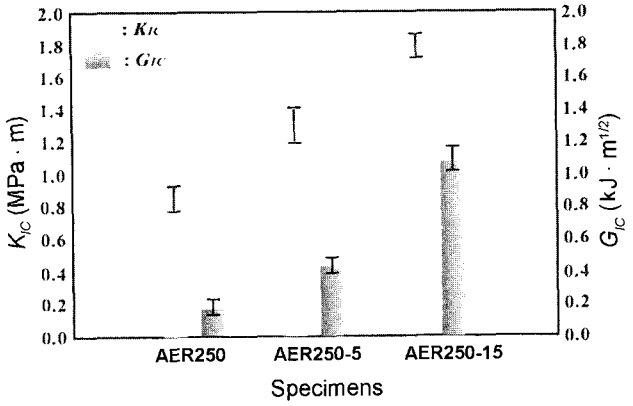

Figure 3. Fracture toughness of neat and rubber-modified epoxy resin.

AER 250 and AER250-5 specimens showed the brittle fracture during linear increase of the load, while AER250-15 specimens showed some ductile and plastic deformation around the maximum load point in advance of the final fracture. The maximum load was used as the critical load, P_C in equation (1). Critical energy release rate G_{IC} was given by

$$G_{IC} = \frac{K_{IC}^2}{E}(1-\nu^2) \quad (2)$$

Figure 3 shows values of K_{IC} and G_{IC} for the neat and rubber-modified epoxy specimens. The more the rubber content, the much larger the amount of K_{IC} and G_{IC}.

Damage Zone Formed Around a Crack Tip

Figure 4 shows the damage zone around a crack tip for the series of AER250 observed by the polarized optical microscope. The arrow in each micrograph indicates a stable crack tip. A large damage zone surrounding the crack was formed in the rubber-modified epoxy resin (see Figure 4(b),(c)), while not in the neat epoxy resin (see Figure 4(a)).

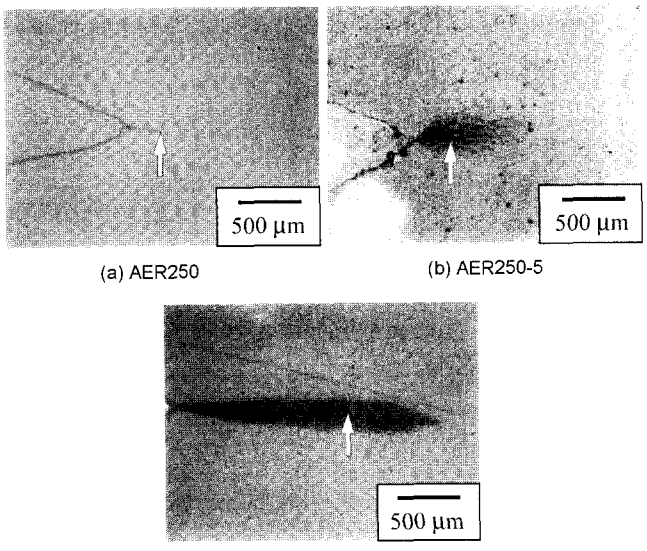

(a) AER250 (b) AER250-5

(c) AER250-15

Figure 4. Damage zones in front of crack tipsobserved by a polarized optical microscope.

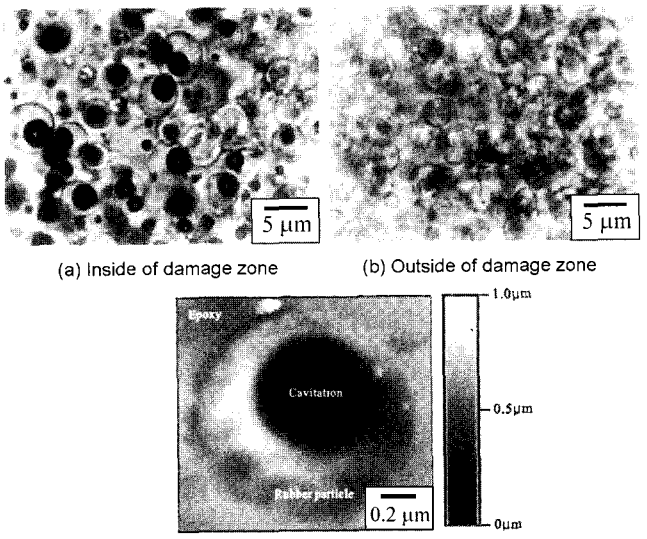

(a) Inside of damage zone (b) Outside of damage zone

(c) Cavitation in rubber particle

Figure 5. Rubber particles inside and outside the damage zone observed by a polarized optical microscope and an atomatic force microscope.

Figure 5(a) and (b) shows the rubber particles inside and outside of the damage zone, as observed by a polarized optical microscope.

Cavitation in rubber particles (see black spots in Figure 5(a)) can be observed in the damage zone. However, no cavitation formed outside of the damage zone. The cavitation and deformation of rubber particles in the damage zone were also confirmed using AFM (Figure 5(c)). The damage zone was generated due to cavitations in rubber particles dispersed in the matrix resin. Cavitation of rubber particles can occur ahead of the crack tip when some hydrostatic tensile stress exceeds a critical value. Cavitation relaxed stresses in the damage zone, causing to increase the deformation and fracture energy and thus the fracture toughness.

Acoustic Emission During Growth Process of Damage Zone

Figure 6 shows typical examples of load and the corresponding hit-event rate as a function of loading time for the specimens of AER250 and AER250-15. In case of AER250, the crack propagated in a very brittle manner at a loading time of 190 sec. Most AE hit-event rates were detected around the fracture point.

Specimen of AER250-5 showed the behavior similar to the case of AER250. In case of AER250-15, however, behavior of AE hit-event rate and the loading curve are divided into

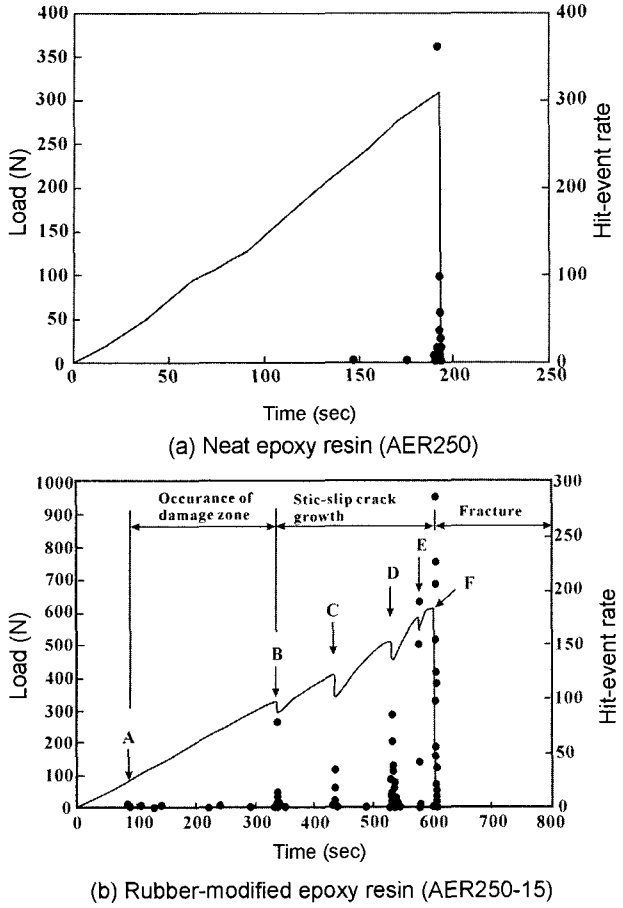

Figure 6. Load and hit-event rate verus loading time for the neat and rubber-modified epoxy resin.

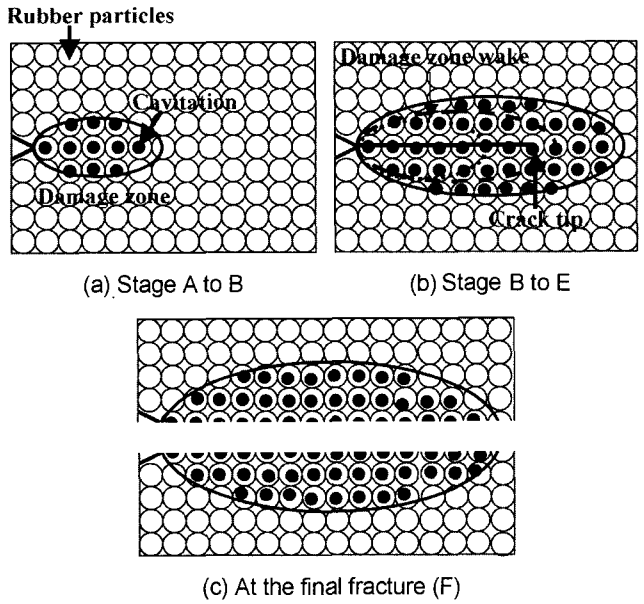

Figure 7. Schematic diagram of the growth of damage zone around crack tips in rubber-modified epoxy resin.

three stages as shown in Figure 6(b). Stage A to B was the begining stage of damage zone as well as cavitation in rubber particles ahead of the pre-crack. The damage zone in this stage was formed without crack initiation by cavitation in rubber particles as shown in Figure 7(a). The AE hit-event rate was in a low level and seemed to be caused by cavitation through the break and/or micro-voids coalescence in rubber particles. AE event rate showed high values probably due to the local fracture of matrix and rubber. During the crack growth from B to F (see Figure 7(b),(c)), some local fracturing proceeded four times generating large AE hit event rate: first at 15 % of the maximum load, second at 75 % , third at 90 % and finally at the maximum load. The crack growth from B to F points showed four times of stick-slip crack propagation behavior [19]. During the load-drop by rapid crack propagation, large hit-event rate was generated.

However, only a few hit-event were defected for the stick period of load increase.

Time-frequency Analysis of AE Signals

Figures 8 and 9 show the results of time-frequency analysis of AE signals from AER250 and AER250-15 specimens, respectively. In case of AER250, frequencies of AE signals were in range of 0.19-0.29 MHz (see Figure 8). In case of AER250-15, on the other hand, AE signals from stage A to B in Figure 6(b) showing the occurence of damage zone formed by cavitation in rubber particles were in ranges of 0.15-0.20 MHz (see Figure 9(a)). Most AE signals from stage B to E in Figure 6(b) showed fraquency range of 0.15-0.30 MHz (see Figure 9(b)). At the final fracture point(F) in Figure 6(b), frequency of AE waves was 0.15-0.30 MHz (see Figure 9(c)). Based on the above frequency analysis, it is thought that AE waves from cavitation were in frequency range of 0.15-0.20 MHz and those from resin crack propagation were in ranges of 0.20-0.30 MHz.

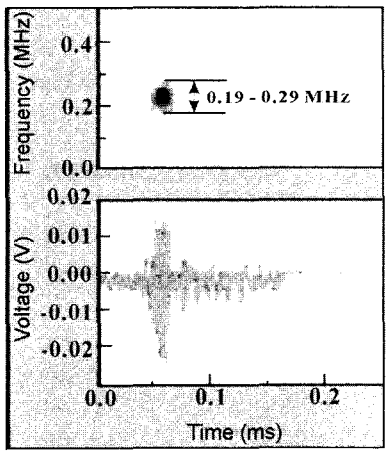

Figure 8. Time-frequency analysis of AE signals measured from neat epoxy resin (AER250).

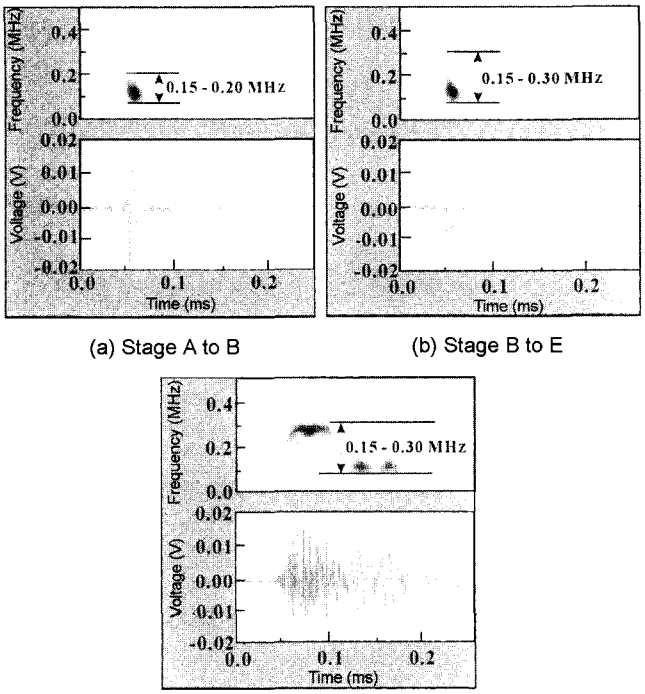

Figure 9. Time-frequency analysis of AE signals measured from rubber-modified epoxy resin.

Conclusions

For the neat and the rubber-modified epoxy resin, we examined the analysis of damage zone around crack tip by acoustic emission. The following conclusions were obtained.

The fracture toughness (K_{IC}, G_{IC}) of rubber-modified epoxy resin increased with increasing rubber contents (wt%).

The damage zone around a crack tip in rubber-modified epoxy resin indicated at about 15 % loading and grew until 57 % loading of the fracture load. The damage zone was formed by cavitation in rubber particles. The crack in rubber-modified epoxy resin initiated at 57 % loading and propagated in a repeated stick-slip manner before the final fracture.

From the time-frequency analysis of AE signal for rubber-modified epoxy resin, AE signals from cavitation were in ranges of 0.15-0.20 MHz and those from crack propagation

Acknowledgements

The author would like to thank to RARC (Reliability Analysis Research Center) in Hanyang Univeristy and MOCIE (Ministry of Commerce, Industry and Energy) for financial support to this work.

References

1. A. F. Yee and R. A. Pearson, *J. Mater. Sci.*, **21**, 2462 (1986).
2. R. A. Pearson and A. F. Yee, *J. Mater. Sci.*, **21**, 2475 (1986).
3. T. K. Chen and Y. H. Jan, *J. Mater. Sci.*, **21**, 111 (1992).
4. H. R. Daghyani, Y. W. Mai, and J. Wu, *J. Mater. Sci. Lett.*, **13**, 1330 (1994).
5. A. J. Kinloch, S. J. Shaw, D. A. Tod, and D. L. Hunston, *Polymer*, **24**, 1341 (1983).
6. W. D. Bascom, *J. Mater. Sci.*, **16**, 2657 (1981).
7. L. T. Manzione and J. K. Gillham, *J. Appl. Polym.*, **26**, 889 (1981).
8. D. B. Lee, *J. Korean Fiber Soc.*, **39**, 430 (2002).
9. D. B. Lee, *J. Korean Fiber Soc.*, **39**, 323 (2002).
10. D. B. Lee, T. Ikeda, M. Todo, N. Miyazaki, and K. Takahashi, *Trans. Japan Soc. Mech. Eng.*, **65**, 25 (1998).
11. D. B. Lee, T. Ikeda, and N. Miyazaki, *The Soc. Mat. Sci. (Japan)*, **50**, 55 (2001).
12. D. B. Lee, T. Ikeda, N. Miyazaki, and N. S. Choi, *Eng. Frac. Mecha.*, **69**, 1363 (2002).
13. D. B. Lee, T. Ikeda, N. Miyazaki, and N. S. Choi, *Trad. ASME J. Eng. Mat. & Tech.*, **124**, 206 (2002).
14. D. B. Lee, T. Ikeda, N. Miyazaki, and N. S. Choi, *J. Mater. Sci. Lett.*, **22**, 229 (2003).
15. R. A. Pearson and A. F. Yee, *J. Mater. Sci.*, **21**, 3828 (1991).
16. R. Bagheri and R. A. Pearson, *Polymer*, **37**, 4529 (1996).
17. A. F. Yee, D. M. Li, and X. Li, *J. Mat. Sci.*, **28**, 6392 (1993).
18. A. S. Holik, R. P. Kambour, S. Y. Hobbs, and D. G. Fink, *Microstructural Sci.*, **7**, 357 (1979).
19. K. Arakawa, T. Mada, and K.Takahashi, *Trans. Japan Soc. Mech. Eng.*, **66**, 883 (2000).